Stability characteristics of a periodically unsteady mixing layer

Muhammad R. Hajj

Citation: Physics of Fluids (1994-present) **9**, 392 (1997); doi: 10.1063/1.869239
View online: http://dx.doi.org/10.1063/1.869239
View Table of Contents: http://scitation.aip.org/content/aip/journal/pof2/9/2?ver=pdfcov
Published by the AIP Publishing

Stability characteristics of a periodically unsteady mixing layer

Muhammad R. Hajj
Department of Engineering Science and Mechanics, Virginia Tech, Blacksburg, Virginia 24061-0219

(Received 9 April 1996; accepted 16 October 1996)

In nature, in many technological applications and in some laboratory experiments, the basic state of shear flows can be time-varying. The effects of such variations on the stability characteristics of these flows are not well understood. In previous work, Miksad *et al.* [J. Fluid Mech. **123**, 1 (1982)] and Hajj *et al.* [J. Fluid Mech. **256**, 385 (1992)], it has been shown that low-frequency components, generated by nonlinear difference interactions, play an important role in the redistribution of energy among spectral components. In particular, phase modulation was found to be the most effective mechanism in energy transfer to the sidebands of unstable modes. In this work, the effects of small-amplitude low-frequency mean flow unsteadiness on the stability of a plane mixing layer are determined. By extending earlier analytical arguments, it is shown that periodicity in the mean flow causes modulations of the most unstable modes. The analysis is then verified experimentally by comparing levels of amplitude and phase modulations in mixing layers with steady and unsteady basic flows. The results show that small-amplitude low-frequency unsteadiness results in enhanced modulations of the fundamental mode. These modulations cause variations in the growth rates of the unstable modes and energy redistribution among them. © *1997 American Institute of Physics.* [S1070-6631(97)01502-X]

I. INTRODUCTION

In the majority of existing studies on the transition to turbulence of shear flows, the mean flow is considered (or assumed to be) steady. Yet, in nature, in many technological applications, and in some laboratory experiments, the mean flow is inherently time-varying. These variations can result from nonuniformities in the external flow field or from self-induced motions of bodies immersed in such a field. In comparison with the stability of shear flows with steady basic states, the stability of unsteady shear flows has received little attention. This is due to many difficulties. Mathematically, the linearized Navier–Stokes equations have coefficients that vary with time and the method of normal modes is not directly applicable. Experimentally, generating well-controlled unsteady mean flow to assess its effects is not easy. In general, the effects of time variations in the basic state on the stability of the flow have been analyzed by applying steady state results to instantaneous velocity distributions, i.e. resorting to the quasi-steady approach. The objective of this work is to examine how small-amplitude low-frequency sinusoidal variations in the mean flow of a plane mixing layer affect its stability.

Shen[1] put forward some ideas on the stability of time dependent flows and explained how the quasi-steady approach is only applicable when the time scale of the unsteady basic flow is very large in comparison to the time scale of the instability disturbances. Shen also showed that for special unsteady basic states, where the steady velocity profile is modified by a temporal function, the solution of the stability problem in the inviscid limit, can be reduced to that of the steady flow by a transformation of the time variable. Davis[2] concluded that for parallel shear flows, and convective and centrifugal instabilities, the stability limits can be modified if mean flow unsteadiness is imposed. Solis *et al.*[3] extended the arguments of Shen to show that mean flow unsteadiness causes amplitude and phase modulations of the instability fluctuations. Through these modulations mechanisms, the mean flow unsteadiness causes acceleration of the transition of a plane wake.

In this work, an experimental investigation is conducted to determine the effects of small-amplitude low-frequency mean flow unsteadiness on the stability characteristics of the plane mixing layer. Interpretation of experimental measurements can be made much easier when they are tied to analytical arguments. In the next section, the analyses presented by Shen and by Solis *et al.* are detailed to show how small-amplitude, low-frequency mean flow unsteadiness causes modulations of the instability modes in the initial linear stage. Time series of velocity fluctuations in a mixing layer with steady and unsteady basic states are then analyzed to substantiate the analytical arguments. In particular, amplitude and phase modulations of instability fluctuations are measured by applying complex demodulation techniques to time traces of velocity fluctuations. The effects of mean flow unsteadiness are isolated by comparing measurements of levels of amplitude and phase modulations and power spectra under the steady and unsteady basic states of the mean flow.

II. STABILITY CHARACTERISTICS OF TIME DEPENDENT FLOWS

Monkewitz and Huerre[4] solved the eigenvalue problem of the linear stability theory that corresponds to different mixing layer velocity profiles. Several experimental studies have shown that linear stability theory is adequate in predicting the frequencies and growth rates of the most unstable modes in steady, incompressible inviscid mixing layers (Ho and Huerre[5]). The application of these results to predict the stability characteristics of mixing layers with an unsteady basic state is not direct. When the flow is unsteady, the coefficients of the governing equations are time dependent and

 1070-6631/97/9(2)/392/7/$10.00

the method of normal modes is not directly applicable. Shen[1] considered the effect of mean flow unsteadiness on the growth of the instability fluctuations for the case where the basic flow is represented as a basic spatial profile, $U(y)$, modified by a time function, $T(t/t_m)$, i.e.,

$$U(y,t)=T(t/t_m)U(y), \tag{1}$$

where t_m is the time scale associated with the basic flow unsteadiness. For the case where $T(t/t_m)$ is given by

$$T(t/t_m)=1+\epsilon e^{i\omega_m t}, \tag{2}$$

the flow would correspond to a mean flow that is subject to an unsteadiness of small amplitude, ϵ, and low frequency, ω_m. By stretching the time variable, a new time scale τ can be defined as

$$\tau=\frac{1}{i\omega_m}\int_0^t(1+\epsilon e^{i\omega_m t})d(i\omega_m t)=t+\frac{\epsilon}{i\omega_m}e^{i\omega_m t}-\frac{\epsilon}{i\omega_m}. \tag{3}$$

Based on this definition, the time derivative $\partial/\partial t$ can be replaced by $T\partial/\partial\tau$. The inviscid linearized differential equation governing two-dimensional streamfunction disturbances then satisfies

$$\frac{\partial}{\partial\tau}\nabla^2\psi+U(y)\frac{\partial}{\partial x}\nabla^2\psi-U''(y)\frac{\partial\psi}{\partial x}=0. \tag{4}$$

Equation (4) is identical to the one obtained under steady basic flow, only with a different time scale, i.e., τ instead of t. Consequently, Eq. (4) can admit solutions of the form

$$\psi=\phi(y)e^{i\alpha(x-c\tau)}, \tag{5}$$

where α is the wavenumber and c is the wave velocity and is taken complex (c_r+ic_i). The real part, c_r, is the phase speed and the imaginary part results in the growth rate, αc_i, when multiplied by α. Using equation (3) and substituting for τ, the following expression for ψ as a function of t is obtained:

$$\psi=\phi(y)e^{(\alpha c_i t+A\cos(\omega_m t+\theta))}e^{i(\alpha(x-c_r t)+A\sin(\omega_m t+\theta))}\times e^{-A\cos\theta}e^{-iA\sin\theta}, \tag{6}$$

where A is equal to $(\alpha\epsilon/\omega_m)(c_i^2+c_r^2)^{1/2}$ and θ is equal to $\tan^{-1}c_i/c_r$. The first exponential term governs the amplitude behavior of the instability mode. The periodic portion of that term, $A\cos(w_m t+\theta)$, implies a modulation of the amplitude of this mode. The second exponential term expresses the wavelike nature of the instability mode and its argument represents the phase. The periodic term in the phase, $A\sin(w_m t+\theta)$, represents a modulation of the phase of the instability mode. The last two terms represent a constant phase shift that may be absorbed in the phase of $\phi(y)$. The experimental work presented next is directed to substantiate the implications of equation (6) that small-amplitude low-frequency variations cause modulations of the unstable modes.

III. EXPERIMENTAL SET-UP AND DATA ANALYSIS

The experiments were conducted in a low-turbulence open return type wind tunnel. The mixing layer was formed by the merging of two laminar streams. The upper and lower free stream velocities were 7.17 m/s and 1.51 m/s, respectively. This resulted in a velocity ratio $R=(U_1-U_2)/(U_1+U_2)=0.65$. The frequency of the dominant instability mode, f_0, is 215 Hz and its streamwise wavelength, λ_0, is 1.98 cm. More details about the wind tunnel and procedures of velocity measurements are given by Hajj *et al.*[6,7] All downstream measurement locations are normalized with R and λ_0, in accordance to our previous work, Hajj *et al.*[6] The test section is isolated from the pump noise by a sonic throat. This arrangement provides an extremely quiet test section flow. The free-stream turbulence intensity is $0.0004U_1$ in the high-speed stream and $0.0008U_1$ in the low-speed stream. This background turbulence is distributed over a broad range of frequency components. The generation of the sinusoidal mean flow unsteadiness simultaneously in both streams was accomplished by varying the cross sectional area of the sonic throat of the tunnel. A brief description of the sonic throat modulator used to produce these variations and its effects on the mean flow are given below.

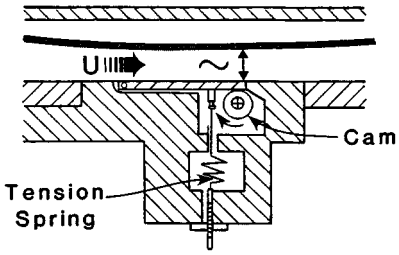

FIG. 1. Schematic of a sonic throat modulator.

The gap of the sonic throat has a height, h, equal to 1.5 cm and a width, w, equal to 10.2 cm. A schematic of the modulator used in these experiments is shown in Fig. 1. The key idea behind the design of this modulator is that changes in the sonic throat flow area have a direct effect on the flow rate in the test section. For a sonic nozzle, the flow rate in the test section can be shown to be linearly proportional to the cross sectional area of the sonic throat. This area is varied by offsetting a hinged flat plate of length $l(=5.1$ cm) with a simple cam. The plate, hinged at the upstream end, is positioned flush to the bottom wall of the sonic throat such that the downstream end of the plate coincides with the location in the sonic-throat which has the minimum mean cross sectional area.

The cam consists of a circular cylinder of radius $r(=6.35$ mm) and an eccentricity $e(=0.09$ mm). The center of rotation is set under the modulator plate by a horizontal distance $z(=6.35$ mm) from end B. The magnitude of throat area variation $|A(t)|$ is adjusted by varying the throw of the cam. As the cam rotates, the free end of the plate periodically constricts the sonic throat. A tension spring is used to keep the plate in contact with the cam. The cam in each case was driven by a 1/4 HP, DC-motor. A transistorized speed controller powered by a power supply was used to set the motor speed. A small flywheel was attached to the cam shaft to stabilize the rotation rate. For a sonic throat of mean vertical opening h and mean cross sectional area A_0, it can be shown

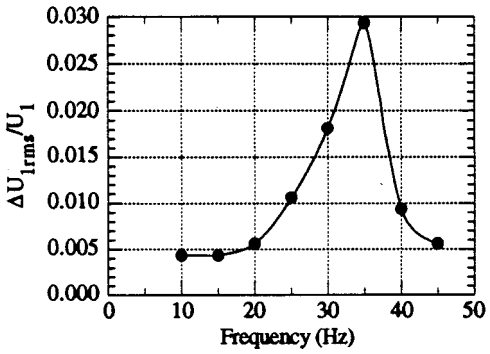

FIG. 2. Normalized rms-amplitude of high-speed mean flow unsteadiness vs frequency at $x=0.0$ cm.

that, because $e/l \ll 1$, $z/l \ll 1$, and $r/l \ll 1$, the throat area varies sinusoidally. For the dimensions presented above, the throat area variation, $A(t)/A_0$ is equal to $e/h(=0.6\%)$.

Measurements of $\Delta U_{1\mathrm{rms}}/U_1$ vs modulator frequency are shown in Fig. 2. Here, $\Delta U_{1\mathrm{rms}}$ is defined as the rms of the mean high-speed velocity variations generated by the sonic throat modulations. The figure shows that these variations are a strong function of the modulator frequency. At the lowest and highest frequencies, $\Delta U_{1\mathrm{rms}}/U_1$ approached 0.5% which is close to e/h. Near the tunnel resonance frequency, i.e., at 35 Hz, $\Delta U_{1\mathrm{rms}}/U_1$ surges to a value near 3%. A time record of the free stream velocity $U_1(t)$ is plotted in Fig. 3(a). The power spectrum of this record is shown in Fig. 3(b). It is obvious that the low-frequency velocity variations, when unsteadiness is imposed, are sinusoidal with an amplitude level that is about two orders of magnitude larger than the background turbulence observed under steady conditions. Note also that the harmonic distortions are at or below background noise level in the tunnel. It is thus clear that the character of mean flow unsteadiness (in frequency and amplitude) is different than that of the background turbulence. Measurements of free-stream velocity in the low-speed side showed the same characteristics as in the high-speed. More specifically, the rms level surged to about 3% at the modulation frequency of 35 Hz and showed a distinct sinusoidal character.

Complex demodulation techniques have been used to determine the levels of amplitude and phase modulations in fluctuating waveforms. Details concerning the complex demodulation procedures can be found in Khadra.[8] Briefly, a modulated time series of the velocity fluctuations can be written in the form

$$u(t)=a(t)\cos(2\pi f_c t+p(t)), \tag{7}$$

where $a(t)$ and $p(t)$ are the amplitude and phase modulations of a carrier wave with frequency f_c. By multiplying Eq. (7) by $2\exp(i2\pi f_d t)$, one obtains

$$a(t)\{\exp[-i2\pi(f_c-f_d)t-ip(t)] + \exp[i2\pi(f_c+f_d)t+ip(t)]\}. \tag{8}$$

The first term includes a difference frequency (f_c-f_d) and the second term includes a sum frequency (f_c+f_d) component. The difference frequency f_c-f_d, can be nullified by

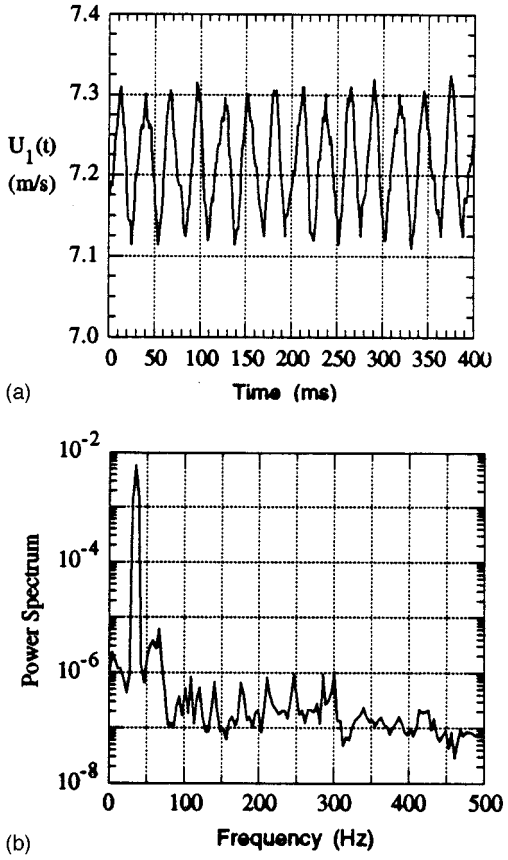

FIG. 3. (a) Sample free-stream time trace. (b) Power spectrum of time trace shown in a.

letting f_d be equal to f_c. The sum frequency component can be eliminated by applying a low-pass filter. The remaining component of the signal is the complex demodulate and is given by

$$c(t)=a(t)\exp[-ip(t)]. \tag{9}$$

The amplitude part of $c(t)$ describes the amplitude modulation of the chosen carrier component f_c. The phase part of $c(t)$ is the phase modulation of that component. From the estimates of the instantaneous amplitude and phase modulations, $a(t)$ and $p(t)$, one can determine other parameters that are related to the physics of the modulated signal. These parameters include the rms amplitude and phase modulation indices defined, respectively, as

$$\hat{\alpha}=\frac{(E[a(t)^2])^{1/2}}{a_0} \tag{10a}$$

and

$$\hat{\beta}=(E[p(t)])^{1/2}, \tag{10b}$$

where $E[\cdots]$ denotes a time average and a_0 is the mean value of $a(t)$. Estimates of these indices will be used to quantify the separate roles of amplitude and phase modulations in the mixing layer under steady and unsteady basic states.

IV. RESULTS AND DISCUSSION

The effects of mean flow unsteadiness on the stability of the plane mixing layer are isolated by comparing measurements and results taken under steady and unsteady basic states. In our previous work on the transition of steady mixing layer, Hajj *et al.*,[6] we showed that the region limited by $Rx/\lambda_0<1.0$ represents the initial stability region. Figure 4 shows the characteristic power spectra measured at four downstream locations in, and just beyond, the initial instability region at the cross-stream location of maximum $u'_{\rm rms}$ when no unsteadiness is imposed. This location was chosen in order to avoid riding up and down a modal profile shape and because, as shown by Miksad,[9] the growth rates of the fundamental and subharmonic modes along maximum $u'_{\rm rms}$ differ only slightly (less than 10%) from those determined by cross-stream integration of total $u'_{\rm rms}$.

At $Rx/\lambda_0=0.32$, the spectra shows the early emergence of a continuous band of instability modes with frequencies up to 250 Hz. At $Rx/\lambda_0=1.0$, the band becomes centered around the most unstable mode with frequency 215 Hz. This mode is referred to as the fundamental mode and will be noted by f_0. A relatively lower peak is also noticed at the mode with frequency equal to half that of the fundamental mode. This corresponds to the subharmonic component, $f_0/2$, whose growth at this early stage is a result of a pressure wave feedback from the vortex pairing mechanism, Corke.[10] Two other peaks also appear at the first and second harmonic, $2f_0$ and $3f_0$, respectively. The enhanced growth of the low-frequency components (up to 50 Hz) should also be noted. The spectrum, at $Rx/\lambda_0=1.3$, is characterized by the enhanced growth of the band of frequencies around f_0, $2f_0$, and $3f_0$, and the emergence of a peak at $4f_0$. The low-frequency components continue to gain energy. These measurements, along with the detailed analysis of Hajj *et al.*,[6] indicate that the $Rx/\lambda_0=1.3$ location marks the beginning of effective nonlinear interactions that result in energy transfer to harmonic bands and low-frequency modes. In this work, we will concentrate on the effects of mean flow unsteadiness in the linear stability region, i.e., $Rx/\lambda_0<1.0$.

Miksad *et al.*,[11] in experimental measurements of a transitioning plane wake, showed that amplitude and phase modulations play an important role in the redistribution of energy to the spectral modes and valleys fill-up. More specifically, those results showed that amplitude and phase modulations provide a very efficient mechanism to achieve spectral energy transfer. Table I shows the amplitude and phase modulation indices, as defined in Eqs. (10a) and (10b), in the natural steady mixing layer for which the spectra is presented above. In this initial stage, up to $Rx/\lambda_0=1.3$, the fundamental mode is the most organized and is the one that is drawing most of the energy from the mean flow. Consequently, it was chosen as the carrier mode. The results show that, in the region up to $Rx/\lambda_0=1.0$, before any strong nonlinear development, the index of amplitude modulation increases significantly while the index of phase modulation remains constant. This indicates the organization of the flow represented by the exponential amplification of the instability modes and especially of the carrier frequency at $f_0=215$ Hz.

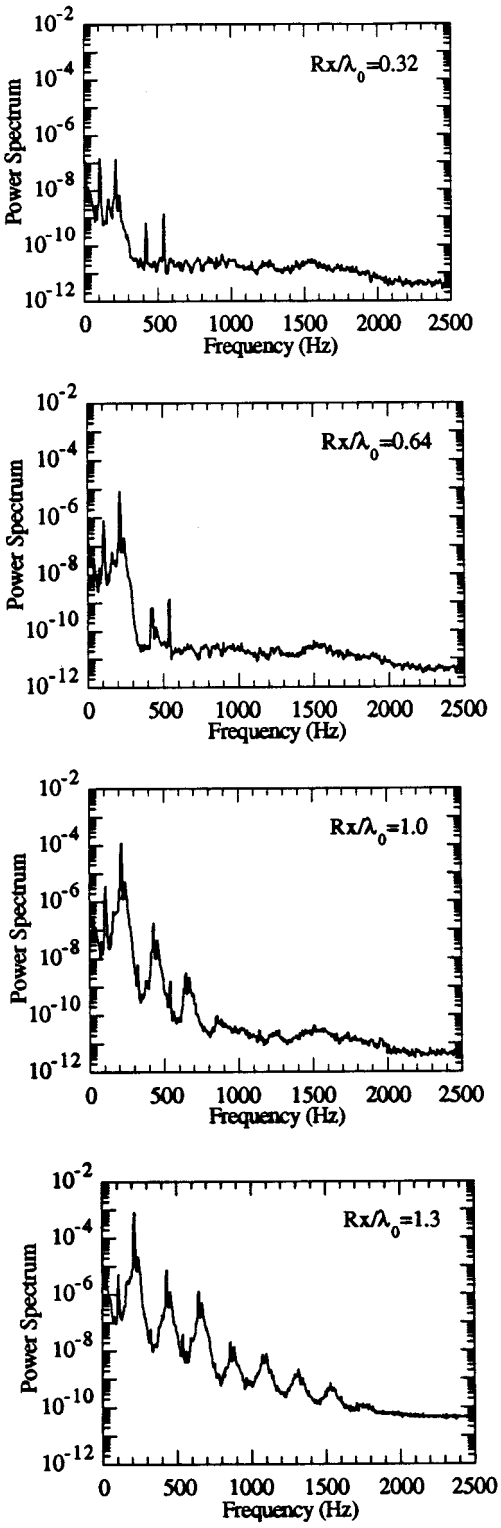

FIG. 4. Power spectra of velocity fluctuations in the steady mixing layer along maximum $u'_{\rm rms}$.

At $Rx/\lambda_0=1.3$, the index of phase modulation increases dramatically while that of the amplitude modulation decreases. This indicates the growing importance of the phase modulation beyond the initial linear instability stage. As seen in the spectrum this location is characterized by enhanced energy transfer to the bands around the most unstable mode and its harmonics. Therefore, the increase in the level of phase

TABLE I. Amplitude and phase modulation indices in the steady mixing layer.

Rx/λ_0	$\hat{\alpha}$	$\hat{\beta}$
0.064	0.489	0.121
0.32	0.504	0.103
0.64	0.751	0.151
1.0	0.9	0.164
1.3	0.738	0.413

modulation is related to the nonlinear activity associated with the energy transfer to the valleys between the spectral peaks.

The effects of mean flow unsteadiness are brought out by comparing measurements taken under steady mean flow conditions, as documented above, to those taken under unsteady mean flow conditions. In both cases, no acoustic forcing is used. Such forcing would have caused enhancement of the excited frequencies as well as other components. For instance, exciting the flow at two modes with a small difference in their frequencies can enhance low-frequency components via difference interactions. Exciting the flow at a frequency near that of the most unstable mode would have a similar effect. Consequently, the natural excitation condition, as considered here, allows the study of effects due strictly to mean flow unsteadiness and comparison with the analytical argument of Sec. II. We should note that while the steady mixing layer is excited by small amplitude and random background fluctuations, the free stream of the unsteady mixing layer shows a clean sinusoidal character as seen in Figs. 3(a) and 3(b). Moreover, because of the experimental setup, both streams undergo the same acceleration and deceleration at all times. Consequently, it is expected that distortions to the mean velocity profile, if there are any, are a part of the effects of the imposed unsteadiness. The effects of mean flow unsteadiness are determined by comparing the indices of amplitude and phase modulations under steady and unsteady mean flow conditions at the same downstream and cross stream locations. Table II shows the values of $\hat{\alpha}$ and $\hat{\beta}$ when unsteadiness is present. The results show that when low-frequency variations are introduced in the mean flow, the amplitude modulation index at $Rx/\lambda_0=0.064$, has a value of 0.717 in comparison to a value of 0.489 measured under steady conditions (Table I). The phase modulation index has a value of 0.579 compared to 0.121 measured under the steady conditions. The enhanced amplitude and phase modulations at $Rx/\lambda_0=0.064$ and 0.32 are in qualitative agreement with the analysis put forward by Shen[1] and Solis *et al.*[3] and detailed in Sec. II. Table II also shows that further downstream, at $Rx/\lambda_0=0.64$ and 1.0, the dynamics and effects of amplitude modulations when the unsteadiness is introduced are different. As discussed above, the amplitude modulation increases and the phase modulation index remains constant over this region, when the basic state is steady. In contrast, when mean flow unsteadiness was introduced, the initially high amplitude modulation decreases while the phase modulation increases. The physical implication is that while the amplitude modulation continues to play its role in transferring energy between the low-frequency and fundamental modes, the enhanced phase modulation allows more mean flow energy to be funneled through the fundamental mode to the sidebands when the mean flow is unsteady. This indicates that the mean flow unsteadiness increases the redistribution of energy among spectral modes.

TABLE II. Amplitude and phase modulation indices in the unsteady mixing layer.

Rx/λ_0	$\hat{\alpha}$	$\hat{\beta}$
0.064	0.717	0.579
0.32	0.665	0.733
0.64	0.531	0.989
1.0	0.415	0.994
1.3	0.254	0.964

A comparison of the power spectra under steady and unsteady mean flow conditions at $Rx/\lambda_0=0.064$, 0.32, 0.64, and 1.0 are shown in Fig. 5. Both spectra show peaks at the frequencies of the fundamental ($f_0=215$ Hz) and subharmonic modes ($f_0/2=107.5$ Hz). Yet, there are several differences. First, the unsteady spectra at all locations show a peak at the frequency of the unsteady component ($f_m=35$ Hz). Second, while the fundamental mode maintains the same amplitude under both steady and unsteady conditions, the subharmonic mode is enhanced significantly by the presence of mean flow unsteadiness. This amplification starts at the first measurement location, $Rx/\lambda_0=0.064$ which corresponds to $x=0.2$ cm. Third, the sideband structures surrounding the fundamental and subharmonic modes are broader under unsteady mean flow than under the steady flow counterpart. Moreover, the spectral valleys, i.e., those regions between the spectral peaks, fill in more rapidly at the successive downstream locations when the mean flow unsteadiness is present. The enhancement of the sideband structure and energy transfer to the spectral valleys is consistent with the enhanced modulations, in particular, phase modulation, by the mean flow unsteadiness as discussed above.

The stability characteristics are best understood by measurements of growth rates in the initial stage of the transition. Figure 6 compares the growth rates of the unstable modes under steady and unsteady mean flow conditions. Although at first sight, both growth rates may appear similar, several significant differences exist. First, the growth rates of the modes with frequencies of 35 Hz (which corresponds to f_m) and 107.5 Hz (which corresponds to $f_0/2$) are enhanced significantly by the presence of mean flow unsteadiness. In conjunction, Fig. 6 also shows that the modes with frequencies near 70 and 140 Hz have higher growth rates due to the presence of mean flow unsteadiness. The enhanced growth rates of all of these modes is accompanied by reduced growth rates of their immediate neighboring modes. These results suggest that the mean flow unsteadiness component can interact with the unstable subharmonic mode and cause the enhanced growth of their sum and difference modes. This interaction mechanism can be explained in terms of amplitude and/or phase modulations of the subharmonic mode by the mean flow unsteadiness, which is consistent with the discussion of Sec. II.

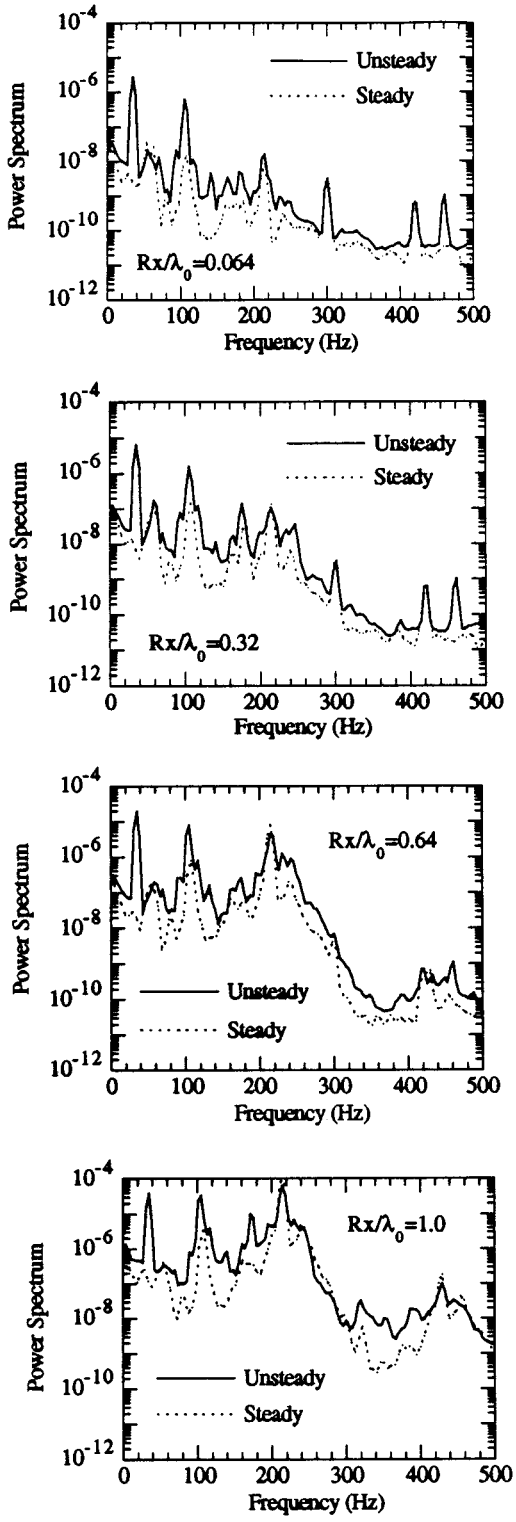

FIG. 5. Comparison of power spectra of velocity fluctuations under steady and unsteady basic states along maximum $u'_{\rm rms}$.

Another feature of the growth rate characteristics of the unstable mode under steady and unsteady mean flow conditions is the enhanced growth of the upper sideband and some modes in the lower sideband of the fundamental mode. These results are consistent with the earlier results in Table II which show enhanced amplitude and phase modulation of the fundamental mode under unsteady mean flow conditions.

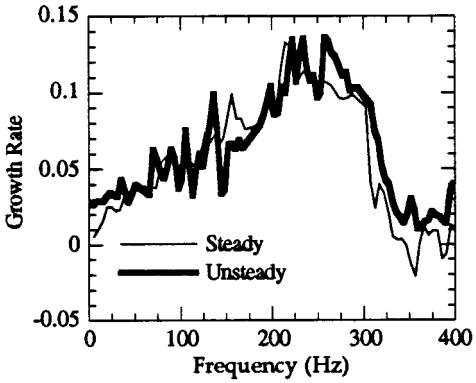

FIG. 6. Normalized growth rates of unstable spectral modes in the mixing layer under steady and unsteady basic states.

It is important to note here that the spacing of the sidebands away from the fundamental are not at integer multiples of f_m as in the case of the subharmonic. This is due to the fact that in contrast with the subharmonic, the band of modes about the fundamental mode are highly unstable also. Within this band, these modes can interact to enhance low-frequency difference modes which in turn cause modulation of the fundamental. Thus, the mean flow unsteadiness acts as an additional modulating frequency of the fundamental and results in significant variations in the growth rates.

V. CONCLUSIONS

In previous work, Miksad *et al.*[11] and Hajj *et al.*,[6] it has been shown that low-frequency components generated by difference interactions among the unstable modes play a special role in the breakdown to turbulence. Through modulations mechanisms, specifically phase modulation, low-frequency components enhance the energy transfer to the sidebands. In this work, the effects of the presence of small-amplitude low-frequency variations in the mean flow on the stability of a plane mixing layer have been examined. By extending the analytical arguments of Shen[1] and Solis *et al.*,[3] it has been shown that such variations cause enhanced modulations of the instability modes. The experimental results support the analytical arguments and show that small-amplitude low-frequency unsteadiness can act as a modulation mechanism. The growth rates of the sum and difference frequency components of the unsteady and subharmonic components increase significantly. Moreover, the enhanced amplitude modulation of the fundamental mode play an important role in passing energy from the low-frequency to spectral modes. On the other hand, the enhanced phase modulation redistributes the energy to the sidebands of the fundamental. In particular, the upper sidebands of the fundamental exhibit higher growth rates than the rates measured under the steady basic state. These results indicate that the breakdown to turbulence may be enhanced by the presence of mean flow unsteadiness.

[1]S. F. Shen, ''Some considerations on the laminar stability of time-dependent basic flows,'' Aerosp. Sci. **28**, 397 (1961).
[2]S. H. Davis, ''The stability of time-periodic flows,'' Annu. Rev. Fluid Mech. **8**, 57 (1976).

[3]R. S. Solis, R. W. Miksad, and E. J. Powers, ''Experiments on the influence of mean flow unsteadiness on the laminar–turbulent transition of a wake,'' *10th Symposium on Turbulence*, edited by X. B. Reed, Continuing Education (The University of Missouri, Rolla, 1985).
[4]P. A. Monkewitz and P. Huerre, ''The influence of the velocity ratio on the spatial instability of mixing layers,'' Phys. Fluids **25**, 1137 (1982).
[5]C. M. Ho and P. Huerre, ''Perturbed free shear layers,'' Annu. Rev. Fluid Mech. **16**, 365 (1984).
[6]M. R. Hajj, R. W. Miksad, and E. J. Powers, ''Subharmonic growth by parametric resonance,'' J. Fluid Mech. **236**, 385 (1992).
[7]M. R. Hajj, R. W. Miksad, and E. J. Powers, ''Fundamental–subharmonic interaction: Effect of phase relation,'' J. Fluid Mech. **256**, 403 (1992).
[8]L. Khadra, ''Digital complex demodulation of nonlinear fluctuation data,'' Ph.D. dissertation, The University of Texas at Austin, 1981.
[9]R. W. Miksad, ''Experiments on the non-linear stages of free shear layer transition,'' J. Fluid Mech. **56**, 695 (1972).
[10]T. C. Corke, ''Measurements of resonant phase locking in unstable axisymmetric jets and boundary layers,'' Nonlinear Wave Interactions in Fluids, The Winter Annual Meeting of ASME, Boston, MA, edited by R. W. Miksad, T. R. Akylas, and T. Herbert, AMD 87, December 1987, pp. 37–65.
[11]R. W. Miksad, F. L. Jones, E. J. Powers, Y. C. Kim, and L. Khadra, ''Experiments on the role of amplitude and phase modulations during the transition to turbulence,'' J. Fluid Mech. **123**, 1 (1982).